On Multidisciplinary Modeling Of The Space Interferometry Mission

Robert L. Grogan
Robert.L.Grogan@jpl.nasa.gov

Robert A. Laskin
Robert.Laskin@jpl.nasa.gov

Jet Propulsion Laboratory
California Institute of Technology
4800 Oak Grove Drive
Pasadena, CA 91109

Abstract

By measuring the positions and motions of stars very precisely, the Space Interferometry Mission (SIM) will produce a wealth of new astronomical data and serve as a technology pathfinder for future astrophysics missions providing a leap forward in space based astronomy beyond the Hubble Space Telescope. SIM will present unprecedented challenges in the measurement and control of distributed optical surfaces mounted on precision space structures, hence driving the technological state-of-the-art in the areas of alignment and stabilization of optical-mechanical systems, deployable structures, vibration isolation and suppression, laser metrology, and the integration and autonomous operation of complex systems.

The precise tolerance required by the SIM instrument facilitates the investigation of many design options, trades, and methods for minimizing interaction between the actively controlled optics and the structure. This paper provides an overview of the multidisciplinary integrated modeling methodology for SIM that encompasses the optics, structures, dynamics, and control disciplines within a common software environment. Such integrated models are used at the Jet Propulsion Laboratory for system requirements trade studies, performance analysis and predictions, and control law design for the mission. The modeling methodology is rooted in a closely tied validation program which is necessary to alleviate the paradox of modeling a spacecraft that does not yet exist. The highest fidelity integrated SIM model to date, examples of utility, and incorporation into the overall instrument design are highlighted.

1.0 Introduction

The Space Interferometry Mission (SIM), with a target launch date of June 2005, will be one of the premiere missions in the Origins Program, NASA's endeavor to understand the origins of the galaxies, of planetary systems around distant stars, and perhaps the origins of life itself. Interferometry is the only known method to significantly improve (by orders of magnitude) the angular resolution of current astronomical telescopes and thereby meet several key scientific goals: measurement of stellar diameters, resolution of close binaries, detection, imaging, and spectroscopy of extra-solar planets, and the precise measurement of galactic and cosmic distance scales. Interferometers lend themselves to space application due to their extremely efficient use of weight and volume to achieve the goals of high resolution, high sensitivity imaging and astrometry. SIM will mark NASA's first scientific use of this revolutionary observing technique in space. If it succeeds, it will presage the flight of the Terrestrial Planet Finder.

Interferometry is the technology of combining the light from spatially distributed small collecting telescope apertures (siderostats) in order to synthesize the resolution of a single large aperture telescope with a diameter equal to the separation distance of the two smaller telescopes. Illustrated in figure 1.1, the SIM design uses three collinear interferometers mounted on a 10-meter long boom. Each interferometer collects light from two siderostats and combines them in the main optics boom. Two of the three interferometers will acquire fringes on bright guide stars in order to make highly precise measurements of the spacecraft attitude. The third interferometer will observe the science targets and measure the target positions with respect to an astrometric grid of some 4000 stars evenly distributed around the celestial sphere.

Since the science object will typically be dim (18-20 magnitude), the attitude information from the two guide interferometers will be used to point the third (science) interferometer and acquire fringes. Using this feedforward technique will allow SIM to rapidly achieve its desired accuracy in position measurements for a single observational period. Note that this requires precise instrument attitude knowledge, not precise attitude control.

An external metrology system measures the three baseline vectors (the distances between the siderostat primary mirrors) from a common reference tetrahedron, and monitors minute changes in the baseline lengths and the relative orientation between the three interferometers. This measurement along with the fringe position information is used to determine the angular separation between stars at the microarcsecond level.

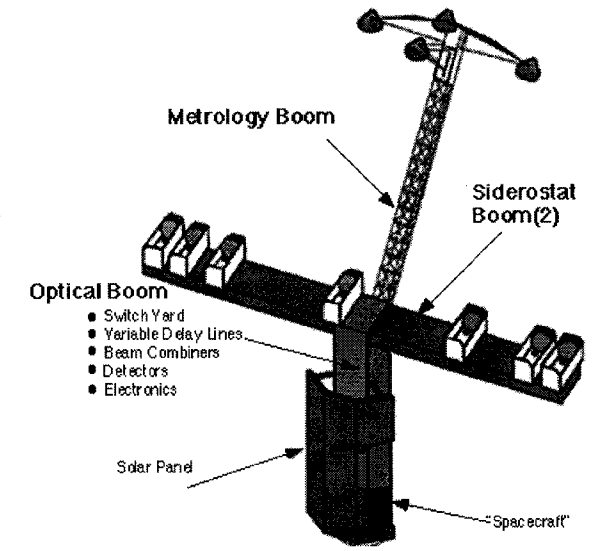

Figure 1.1: SIM Spacecraft Configuration

Control requirements are driven by requirements on fringe visibility for astrometry and imaging as well as by the requirement for starlight nulling. The nulling requirement is the more stringent necessitating 1 nanometer RMS optical path difference (OPD) control over a broad frequency range. Fringe visibility requirements translate into the need for 10 nanometer RMS OPD control at frequencies above the fringe detector frame rate of approximately 1 kHz and more relaxed requirements at lower frequencies.

The complexity of an interferometer, with all its moving parts and control systems, is the price that must be paid for stepping beyond the paradigm of rigid monolithic telescopes as built since the days of Galileo. In order to achieve these requirements multi-layered broadband control is employed using active optics (controlling 50 optical degrees of freedom), active and passive vibration isolation, and structural damping leading to a large number of actuators and sensors distributed across a lightly damped lightweight flexible structure having high modal density.

2.0 Building the Integrated Model

An integrated spacecraft model has been built to be parameterized in frequency by certain key defining features of the instruments ultimate performance. These features may by categorized into four classes: gross structure, components, control loop bandwidths, and disturbances. Figure 2.1 shows a preliminary frequency domain layout of the critical parameters in these four classes. The philosophy here is to use engineering judgement to decouple dynamics in the frequency domain by carefully separating critical modes, disturbance spectrums, and control loop bandwidths. Traditionally dynamics and control design would then proceed by analyzing component models of the reference design. A departure from tradition must be taken for a complex integrated spacecraft and instrument such as SIM. A multidisciplinary (structures, optics, dynamics, and control) model has been created to validate engineering judgement of the reference design, navigate the large complex trade space, and establish requirements on the parameterized classes of critical parameters. Integral to defining a methodology for the creation of such a model is a case study validation activity using a ground-based full-scale dynamically and dimensionally representative hardware model of a space interferometer called the Micro-Precision Interferometer (MPI) located at JPL [1].

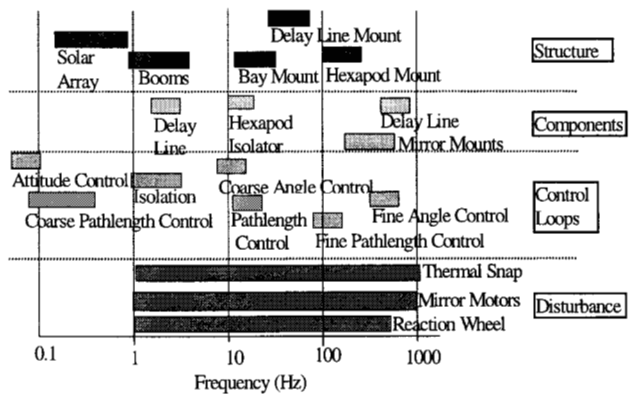

Figure 2.1: Frequency Domain Mapping

2.1 Structural Model

The structural model of the spacecraft was constructed completely within the Matlab environment using the Integrated Modeling of Optical Systems (IMOS) toolbox developed at JPL [2]. IMOS enables end-to-end modeling of complex optomechanical systems (including optics, controls, structural dynamics, and thermal analysis) in a single seat workstation computing environment. IMOS also incorporates several graphics functions that enable viewing of the structural assembly, structural deformations, and element optical layouts. IMOS has been applied at JPL to the Hubble Space Telescope and the Space Infrared Telescope Facility (SIRTF), as well as virtually all the space interferometer designs that have been considered in recent years. Currently IMOS is the baseline integrated modeling tool for the SIM project and NGST pre-project, and is also being adopted by their industrial partners.

Euler beam elements model the three instrument booms (siderostat, metrology, and optics). The siderostat boom supports seven bays each holding four mirrors including a collecting aperture. Several fold mirrors in the optical layout are attached using rigid body elements. The optics boom supports eight optical delay lines (four active and four passive), four beam combiners, and sets of switch-yard mirrors. Grid points are defined at optics mount locations to be consistent with the optics layout described below. Complex optics bay mounts have been replaced by six degree of freedom stiffness and mass matrices via modal reduction of high fidelity IMOS or NASTRAN finite element models. Portions of the model have been correlated with brassboard level hardware components build for the JPL Interferometry Technology Program. Figure 2.2 illustrates the finite element model geometry.

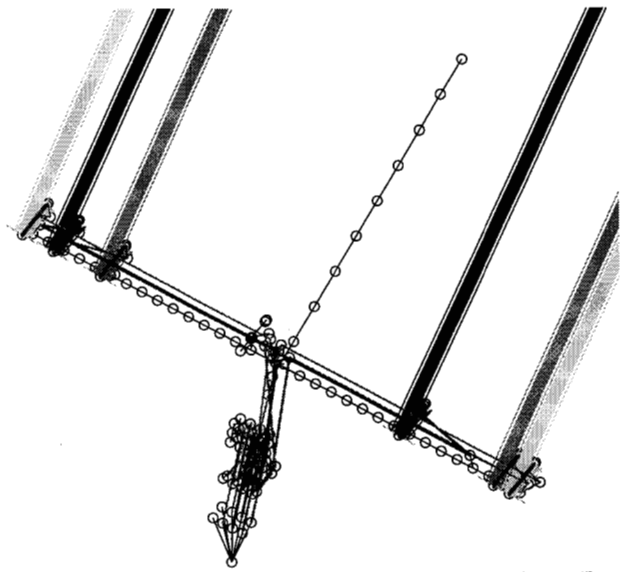

Figure 2.2: SIM Finite Element Model With Optical Ray Trace

The resulting model has 1200 independent degree of freedom and is of the form:

$$M\ddot{d} + Kd = Bf \qquad (2.1)$$

where M is the global mass matrix, K is the global stiffness matrix, B is the force influence matrix, d is the nodal displacement vector, and f is the force vector.

The eigen-solution is found such that

$$\left(K - \Omega^2 M\right)\Phi = 0 \qquad (2.2)$$

where Φ are the component Ritz vectors or mode shapes and Ω are the eigenvalues or system natural frequencies.

By defining the transformation to the set of generalized coordinates, q, such that $d=\Phi q$. The equations of motion for the finite element model can be written as:

$$\ddot{q} + 2Z\Omega\dot{q} + \Omega^2 q = \Phi^T Bf \qquad (2.3)$$

forming a set of inertially and elastically uncoupled independent equations of motion. The damping term $2Z\Omega\dot{q}$ is added to introduce modal damping on selected modes. The modes above 1000 Hz are truncated resulting in a system of 108 modes.

2.2 Optical Model

The optical model is created using IMOS, as well as, a Matlab mex-file version of MACOS (Modeling and Analysis for Controlled Optical Systems) also developed at JPL [3].

The instrument optical layout is used to describe the system optical prescription defining the location, orientation, and shape of the optical elements. Each optical element location is consistent with a finite element grid point. Using this prescription a linear optical model is generated. The linear optical model provides a linear coordination transformation from nodal displacement (translation and rotation) to optical ray perturbation as described by equation 2.4. This linear transformation matrix is called the optical sensitivity matrix.

$$y_{opt} = C_{opt} d \qquad (2.4)$$

where y_{opt} is the vector of optical metrics which may be optical pathlength, wavefront tilt, or spot motion on a detector, and C_{opt} is the optical sensitivity matrix.

Optical performance in interferometry is typically measured in terms of optical pathlength difference (OPD) and differential wavefront tilt (DWT). The linear transformation from nodal displacement to optical pathlength and wavefront tilt is calculated for each of the six telescopes and the appropriate terms of the optical sensitivity matrix are subtracted for the telescope pairs forming the three interferometer baselines. Figure 2.2 illustrates the optical model ray trace on the SIM finite element geometry.

2.3 Integrated Model

The linear finite element model and linear optical model are integrated in state space form such that:

$$\begin{aligned} \dot{x} &= Ax + Bu \\ d &= Cx \end{aligned} \qquad (2.5)$$

where

$$A = \begin{bmatrix} 0 & I \\ -\Omega^2 & -2Z\Omega \end{bmatrix} \quad B = \begin{bmatrix} 0 \\ B_o \end{bmatrix} \quad C = [C_1 \quad 0]$$

$$B_o = \Phi^T B \quad \text{and} \quad C_1 = C_{opt}\Phi$$

Inputs are defined at disturbance locations and actuated degrees of freedom for the articulated optical surfaces of the delay lines and fast steering mirrors. Output optical metrics are starlight and internal metrology optical pathlength difference (OPD) for the three interferometer baselines; wavefront tilt for the three interferometer baselines; and rigid body attitude and rate.

2.3 Control Model

Actuators have been modeled with one free and one attached coincident nodes connected by an elastic element representing the flexure mount. In total there are seven tip-tilt fast steering mirrors used for wavefront tilt correction and three active delay lines used for pathlength control.

Each delay line has three actuators: a voice coil supporting a primary mirror used for low bandwidth control and two piezoelectric transducers (one supporting a small secondary mirror and a second to momentum compensate the first) providing high bandwidth optical pathlength control. Inputs are also provided at the reaction wheel mount location for disturbance injection and a linear rigid body control loop.

Active optics loops were designed using classical bode loop shaping techniques for single input / single output systems. Linear compensators are represented in state space form. Loop gains and bandwidths are based on instrument observational requirements and are consistent with those achieved in ground testbeds. A block diagram of the integrated model is shown in figure 2.3.

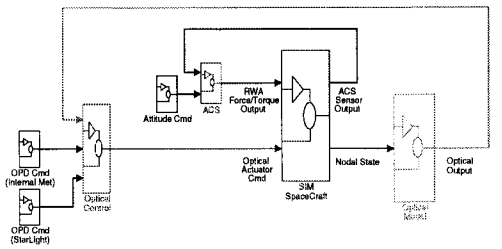

Figure 2.3: Block Diagram

2.4 Disturbance Model

The most significant periodic disturbance on board the spacecraft will likely be the reaction wheel assembly (RWA) used for attitude control. The baseline SIM architecture uses a pyramid array of four RWA's. It can be shown [4] that the force and torque disturbance, m, originating from static and dynamic unbalance of a RWA can be modeled as the summation over i of n discrete sinusoidal harmonics, h_i, of the RWA rotation rate, f_{RWA}, with amplitude proportional to the rotation rate squared as given in equation 2.6.

$$m(t) = \sum_{i=1}^{n} A_i f_{RWA}^2 \sin\left(2\pi h_i f_{RWA} t + \phi_i\right) \qquad (2.6)$$

where A is the harmonic amplitude coefficient and ϕ is a random phase angle.

The A_i and h_i terms are determined experimentally and are unique for a given RWA. In this paper the disturbance model is based on Hubble Space Telescope RWA flight unit test data [5]. Axial and radial force disturbances, as well as, wobble torque disturbance about the radial axis are modeled. Test data indicates that torque disturbance about the axial or spin axis due to ripple and cogging effects is negligible.

In order to facilitate broadband frequency domain design and analysis a stochastic broadband RWA model was generated in reference [4] with the assumption that the wheel speed is a uniform random variable over the interval 0 to 3000 RPM (the expected operating range). Figure 2.4 shows the power spectral density (PSD) functions for the three axes of disturbance for a single RWA.

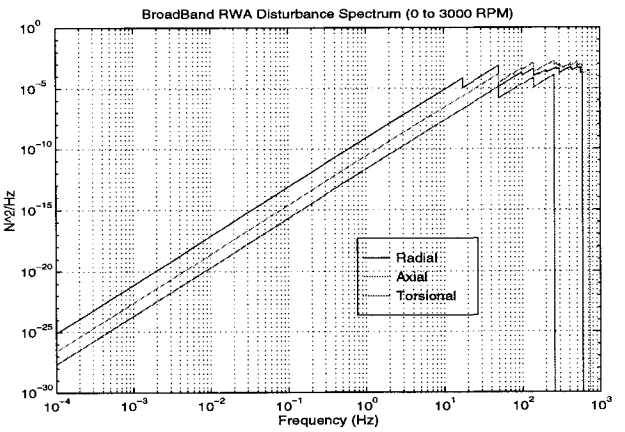

Figure 2.4: RWA Broadband Disturbance PSD

3.0 Case Study For Spacecraft/Instrument Design

As stated above the spacecraft/instrument model has been built to contain physically identifiable parameters that may be traced to requirements on critical features. The utility of such a model is two fold. First for the mission requirements definition and design phase the model may be used to establish and validate design spectrum requirements on critical features including optics mounts, component mounts, gross structure, control bandwidths, and disturbance sources. Secondly, as the detailed design solidifies and the model gains the required complexity it may be used for performance prediction. This performance assessment includes items such as the end-to-end optical pathlength performance analysis from disturbance to fringe visibility for guide and science baselines and end-to-end pointing performance analysis from disturbance to wavefront tilt for guide and science baselines.

Consider the following case study of navigating the trade space for defining a requirement on RWA disturbance isolation (note: this case study will be restricted to results from a single guide star baseline with the optical control loops closed. By looking at the RWA disturbance PSD, engineering judgement may select the RWA to be isolated in six degrees of freedom using a hexapod with a bounce mode break frequency of 10 Hz. Thus, isolating the disturbance transmission above 10 Hz and also being a relatively easy component to build (cost and complexity increase with lower frequency). Luckily, the component actually exists and a simplified model of the hexapod is integrated into the system model.

The transfer functions from the six degrees of freedom RWA mount location to OPD for the guide star baseline are calculated. Figures 3.1 and 3.2 show the effect of isolation on the three force components magnitude frequency response for the model without and with the hexapod, respectively.

Reference [6] derives the following equation for modal ranking or modal gain σ^2:

$$\sigma_i^2 = \frac{\left[b_{oi} b_{oi}^T c_{1i}^T c_{1i}\right]^{\frac{1}{2}}}{4\zeta_i \omega_i^2} \qquad (3.1)$$

where σ_i is the modal influence coefficient or modal gain of the i^{th} mode, b_{oi} is the i^{th} element of B_o, c_i is the i^{th} element of C_1, ω_i is the i^{th} diagonal element of Ω, ζ_i is the i^{th} diagonal element of Z.

The modal gains from the root sum square (RSS) of the six axes of RWA disturbance input to the OPD metric are calculated, normalized, and plotted in figure 3.3. Four modes just above 10 Hz have the largest modal participation, as well as, a few modes between 5 and 20 Hz. By means of mode shape visualization these particular modes are found to be the hexapod itself, as well as, coupled modes of the large support booms and collecting aperture bay mounts to the support booms.

The broadband RWA disturbance PSD is convolved with the disturbance to OPD transfer function via the following equation:

$$\Phi(\omega)_{OPD} = \left| G(j\omega)_{\frac{OPD}{RWA}} \right|^2 \Phi(\omega)_{Disturbance\,RWA} \qquad (3.2)$$

where $G(j\omega)$ is the RWA disturbance to OPD transfer function and $\Phi(\omega)$ is a broadband power spectral density function. The resultant PSD of OPD is shown in figure 3.4. The variance of OPD is calculated by integrating this PSD over the frequency range from 0 to 1 kHz. Total RMS OPD for the guide baseline of interest is calculated to be 1.2 nm, thus greater than the 0.44 nm allocated to RWA induced OPD jitter for the nulling requirement error budget. Thus, a 10 Hz isolation corner frequency proves not to be a good design selection.

Further exploration of the isolation frequency trade space gives the series of PSD's parameterized by corner frequency (1, 2, 5, 10, and 20 Hz) which are shown in the waterfall plot in figure 3.5. Note that here only the frequency range from 5 to 25 Hz is shown since figure 3.4 indicates that this is the range where there is energy above the line drawn as the 0.44 nm requirement.

The RMS OPD is calculated for each isolation frequency case as well as, for the parameterized structure modal damping (0.1, 0.5, 1, 2, 3, and 5 %). The resulting surface is shown in figure 3.6. As illustrated by this plot at 0.1% structural damping the requirement is met by a factor of 3 for the isolation frequencies 5 Hz and lower. The plot also shows that perhaps a similar result can be reached by taking steps to increase structure damping if less than 10 Hz isolation turns out to be undesirable. Of course, cost and complexity also increasing with greater damping.

The modal gain analysis provided information that there are a set of coupled modes very near the 10 Hz isolation frequency. Perhaps establishing a set of requirement restricting the range of the support boom or component mount modes is a better solution. There may also be countless other solution spaces to be explored via the multidisciplinary model of SIM.

4.0 Summary and Future Direction

SIM will drive the state-of-the-art in optomechanical and optoelectronic systems as well as present daunting challenges in precise stabilization of lightweight deployable structures and coordinated computer control of numerous optical surfaces. Integrated modeling has proven to be a valuable tool for navigating the rather complex trade space of dynamics and control spacecraft/instrument requirements for the mission. This paper presents simply an overview of the methodology that shall be used for the design and performance prediction of the flight instrument.

5.0 Acknowledgements

The work described in this paper was carried out at the Jet Propulsion Laboratory, California Institute of Technology, under contract with the National Aeronautics and Space Administration.

6.0 References

[1] Melody, J. W., and Neat, G. W., "Integrated Modeling Methodology Validation Using The Micro-Precision Interferometer Testbed," Proc. 35th IEEE Conference on Decision and Control, Kobe, Japan, Dec. 1996.

[2] Integrated Modeling of Optical Systems User's Manual, Release 3, 1998, Jet Propulsion Laboratory. (Internal Document)

[3] Modeling and Analysis for Controlled Optical Systems User Manual, Jet Propulsion Laboratory, 1997. (Internal Document)

[4] Melody, J. W., "Discrete-Frequency and Broadband Reaction Wheel Disturbance Models," Interoffice Memorandum, Jet Propulsion Laboratory, June 1995. (Internal Document)

[5] Hasha, M., D., "Reaction Wheel Mechanical Noise Variations," Lockheed Martin, EM SS 218, June 1986.

[6] Gregory, C. Z., "Reduction of Large Flexible Models Using Internal Balancing Theory," Journal of Guidance, Control, and Dynamics, Vol.7, No. 6, 1984.

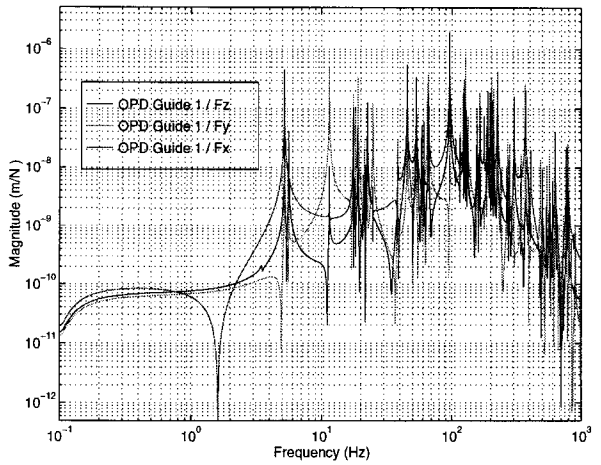

Figure 3.1: RWA Disturbance to OPD Frequency Response (No Isolation)

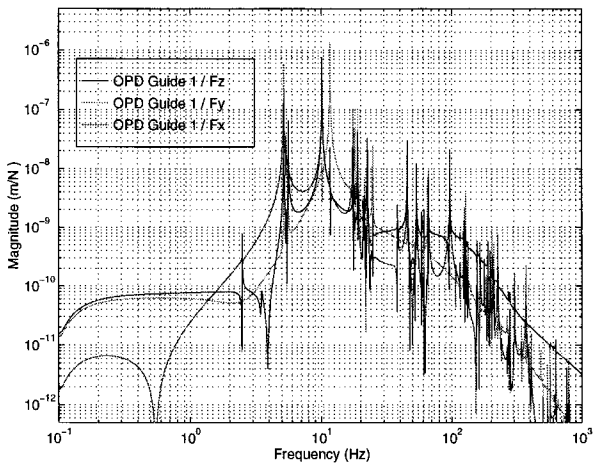

Figure 3.2: RWA Disturbance to OPD Frequency Response (10 Hz Isolation)

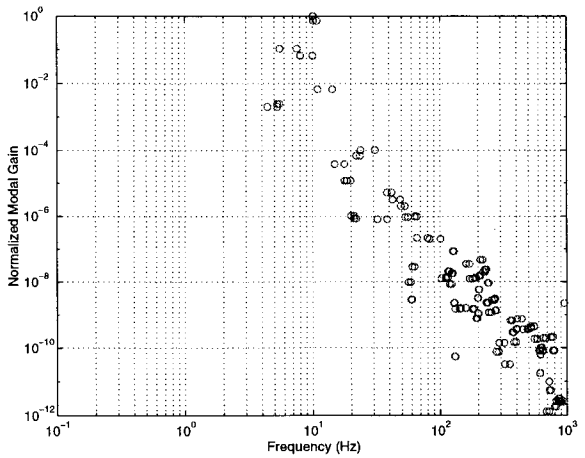

Figure 3.3: Modal Gain From RWA to OPD (10 Hz Isolation)

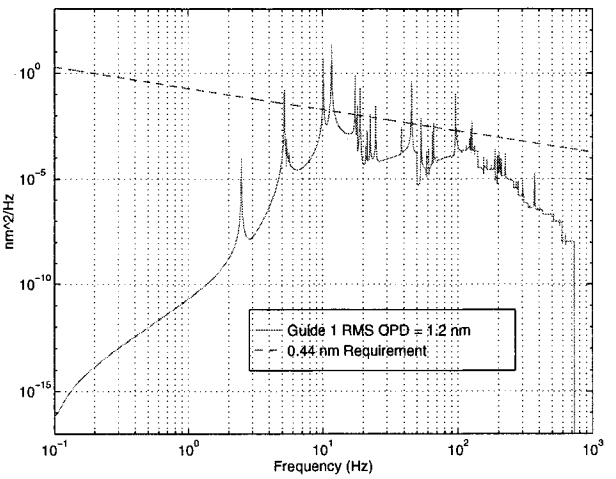

Figure 3.4: Stellar OPD PSD (10 Hz Isolation)

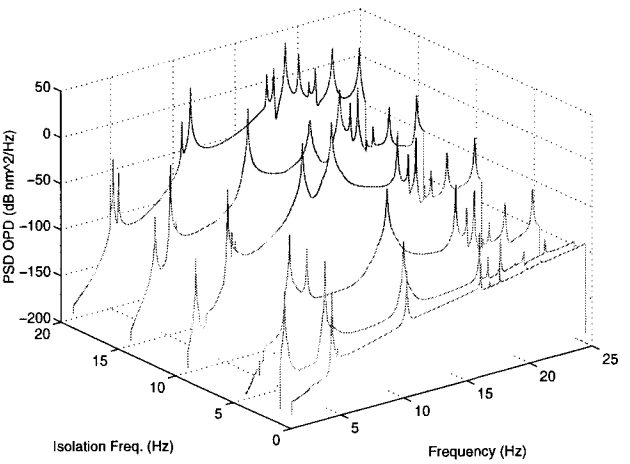

Figure 3.5: Stellar OPD PSD Variation With Isolation Frequency

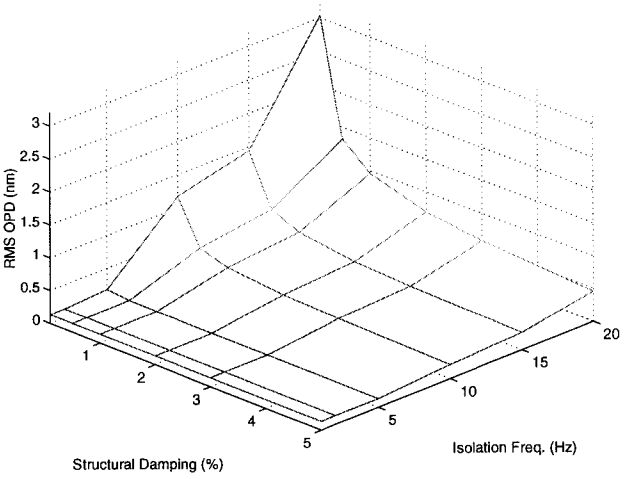

Figure 3.6: RMS Stellar OPD Variation With Isolation Frequency and Structural Damping (Closed Loop Optics)